1892 *Chem. Mater.* **2010,** *22,* 1892–1900
DOI:10.1021/cm9034374

CHEMISTRY OF MATERIALS
Article

Structural Polymorphism in Li_2CoSiO_4 Intercalation Electrodes: A Combined Diffraction and NMR Study

A. Robert Armstrong,[†,§] Christopher Lyness,[†,§] Michel Ménétrier,[‡,§] and Peter G. Bruce*[,†,§]

[†]*EaStCHEM, School of Chemistry, University of St. Andrews, St. Andrews, Fife KY16 9ST, U.K.,* [‡]*ICMCB-CNRS, 87 Av. Schweitzer, 33608 Pessac, France, and* [§]*Alistore European Research Institute, 33 Rue Saint Leu, 80039 Amiens Cedex, France*

Received November 11, 2009. Revised Manuscript Received January 7, 2010

Li_2CoSiO_4 was prepared in three polymorphic forms. The β_{II} ($Pmn2_1$) polymorph was obtained by hydrothermal synthesis (150 °C), and subsequent heat treatments yielded the β_I ($Pbn2_1$) form (700 °C) and the γ_0 ($P2_1/n$) form (1100° then quenching from 850 °C). Rietveld refinement of X-ray and neutron powder diffraction patterns reveal considerable Li/Co mixing for β_{II}, very moderate mixing for β_I, and no mixing for γ_0. ^{7}Li MAS NMR spectra have been recorded for the three forms. The mechanism of the Fermi contact interaction that leads to negatively shifted signals is as yet unexplained, but the nature and the number of signals were analyzed in relation to the site occupancies for each compound. The agreement is good for β_{II}, although the extent of disorder leads to very poorly defined NMR signals; it is reasonable (although not fully quantitative) for β_I, where well-defined NMR signals can be assigned to definite environments; finally, the γ_0 sample surprisingly leads to a single rather broad NMR signal, whereas two well-defined and rather different environments are present in the structure deduced from diffraction.

Introduction

New batteries are needed urgently to meet the demands of modern technology and to address the challenge of Global Warming. The layered Li intercalation compound, $LiCoO_2$, is used as the cathode in the majority of commercial rechargeable lithium-ion batteries.[1,2] A number of alternative layered compounds, such as $LiNiO_2$ or $LiMnO_2$, have also been considered: their solid solutions, such as $Li(Co_{1/3}Mn_{1/3}Ni_{1/3})O_2$, are used in the latest commercial products.[3−5] Retention of some Co is important in achieving good cathode performance. The recognition that compounds containing the phosphate anion, such as the olivine $LiFePO_4$, could act as lithium intercalation hosts and thus operate as cathodes in rechargeable lithium batteries, represented a significant breakthrough.[6] Bonding of the oxygen to the phosphorus stabilizes the former with respect to evolution from the structure, an important problem on charging simple transition metal oxides. Recently, an entirely new class of lithium intercalation compounds based on silicates, Li_2MSiO_4, where M = Fe, Mn, Co, has been described.[7] Of these the most studied is Li_2FeSiO_4; it has been shown that at 60 °C, 165 $mAhg^{-1}$ of charge may be extracted, equivalent to 1 lithium per formula unit; with reversible lithium cycling over the range Li_xFeSiO_4, $1.15 < x < 2$, corresponding to 140 $mAhg^{-1}$ when suitably carbon coated and with a particle size of <150 nm.[7a] In this paper we focus on Li_2CoSiO_4.

The Li_2MSiO_4 compounds (M = Fe, Mn, Co) belong to a large family of materials known as the tetrahedral structures.[8] Generally the tetrahedral structures are composed of tetragonally packed oxide ions (a distorted form of hexagonal close packing) within which half the tetrahedral sites are occupied by cations, such that face sharing between the pairs of tetrahedral sites is avoided.[9] These

*Corresponding author e-mail: pgb1@st-and.ac.uk.

(1) Mizushima, K; Jones, P. C.; Wiseman, P. J.; Goodenough, J. B. *Mater. Res. Bull.* **1980**, *15*, 783.
(2) Nagaura, T. Paper presented at 4th Int. Rechargeable Battery Seminar, Deerfield Beach, FL, 1990. Nagaura, T.; Tazawa, K. *Prog. Batteries Col. Cells* **1990**, *9*, 20.
(3) (a) Li, W.; Reimers, J. N.; Dahn, J. R. *Solid State Ionics* **1993**, *67*, 123. (b) Rougier, A.; Gravereau, P.; Delmas, C. *J. Electrochem. Soc.* **1996**, *143*, 1168.
(4) Armstrong, A. R.; Bruce, P. G. *Nature* **1996**, *381*, 499.
(5) (a) Yabuuchi, N.; Ohzuku, T. *J. Power Sources* **2003**, *119−121*, 171. (b) Jouanneau, S.; Eberman, K. W.; Krause, L. J.; Dahn, J. R. *J. Electrochem. Soc.* **2005**, *150*, A1637.
(6) (a) Padhi, A K.; Nanjundaswamy, K. S.; Goodenough, J. B. *J. Electrochem. Soc.* **1997**, *144*, 1188. (b) Padhi, A K.; Nanjundaswamy, K. S.; Masquelier, C.; Okada, S.; Goodenough, J. B. *J. Electrochem. Soc.* **1997**, *144*, 1609. (c) Yamada, A.; Chung, S. C.; Hinokuma, K. *J. Electrochem. Soc.* **2001**, *148*, A224. (d) Chung, S. Y.; Bloking, J. T.; Chiang, Y. M. *Nat. Mater.* **2002**, *1*, 123. (e) Herle, P. S.; Ellis, B.; Coombs, N.; Nazar, L. F. *Nat. Mater.* **2004**, *3*, 147.
(7) (a) Nytén, A.; Abouimrane, A.; Armand, M.; Gustafsson, T.; Thomas, J. O. *Electrochem. Commun.* **2005**, *7*, 156. (b) Dominko, R.; Bele, M.; Gaberscek, M.; Meden, A.; Remskar, M.; Jamnik, J. *Electrochem. Commun.* **2006**, *8*, 217. (c) Gong, Z. L.; Li, Y. X.; Yang Y, Y. *Electrochem. Solid-State Lett.* **2006**, *9*, A542. (d) Arroyo de Dompablo, M. E.; Armand, M.; Tarascon, J. M.; Amador, U. *Electrochem. Commun.* **2006**, *8*, 1292. (e) Wu, S. Q.; Zhang, J. H.; Zhu, Z. Z.; Yang, Y. *Curr. Appl. Phys.* **2007**, *7*, 611. (f) Masquelier, C.; , Quoirin, G.; , Dupont, L.; Taulelle, F. Proceedings of International Meeting on Lithium Batteries, Biarritz, **2006**. (g) Lyness, C.; Delobel, B.; Armstrong, A. R.; Bruce, P. G. *J. Chem. Soc., Chem. Commun.* **2007**, 4890.
(8) (a) West, A. R.; Glasser, F. P. *J. Solid State Chem.* **1972**, *4*, 20. (b) Tarte, P.; Cahay, R. *C. R. Acad. Sci. Paris C* **1970**, *271*, 777.
(9) Bruce, P. G.; West, A. R. *Acta Crystallogr., Sect. B: Struct. Crystallogr. Cryst. Chem.* **1982**, *38*, 1891.

 Published on Web 01/25/2010

tetrahedral structures exhibit a rich polymorphism, with more than 8 different polymorphs known. They may be divided into two families, designated β and γ. In the case of the former all the tetrahedra point in the same direction, perpendicular to the close-packed planes, and share only corners with each other. In the case of the γ polymorphs, the tetrahedra are arranged in groups of three with the central tetrahedron pointing in the opposite direction to the outer two, with which it shares edges. Where both β and γ polymorphs exist for a given compound the latter is stable at higher temperatures, with the β to γ transformation involving inversion of half the tetrahedral sites.[10] Several variants of both β and γ exist, involving either ordering or distortions of the parent structures; they are designated β_I, γ_0, γ_{II}, etc. In many instances these phases may be quenched to room temperature, where they exhibit long-term stability. Originally the different polymorphs were distinguished only on the basis of differences in their powder X-ray diffraction patterns.[8a] More recently, the complete crystal structures of a few isolated examples have been solved.[11]

As a result of the complex polymorphism exhibited by the tetrahedral structures it is beneficial, when studying the structures of these materials to employ techniques that probe both short- and long-range structure. Magic angle spinning NMR was chosen as a probe of the local structure since it was shown to be very powerful in assessing the purity of high-pressure treated Li_2MnSiO_4 ($Pmn2_1$), characterized by a well-defined single type of Li.[12] Since Li is a weak scatterer of X-rays, neutron powder diffraction was chosen to investigate the long-range structure in three polymorphs of Li_2CoSiO_4.

Experimental Section

The β_{II} polymorph was prepared by hydrothermal synthesis. $LiOH \cdot H_2O$ (0.05 mol) (Aldrich) was added to 0.0125 mol of SiO_2 (Aldrich) in 20 mL of distilled water and stirred. $CoCl_2$ (0.0125 mol) (Aldrich) was added to 10 mL of ethylene glycol and stirred under gentle heat until dissolution occurred. The two solutions were then mixed with stirring, and the slurry was transferred to a 40 mL Teflon-lined autoclave. The remaining volume was topped up with distilled water. The sealed autoclave was heated at 150 °C for 72 h. The product was filtered and dried at 60 °C overnight.

The β_I form was obtained by heating the β_{II} phase in air to 700 °C for 2 h. The γ_o phase was formed by heating the β_{II} polymorph to 1100 °C for 2 h and then lowering the temperature to 850 °C whereupon the material was quenched to room temperature.

Powder X-ray diffraction data were collected on a Stoe STADI/P diffractometer operating in transmission mode with $FeK\alpha_1$ radiation (λ = 1.936 Å) to eliminate Co fluorescence.

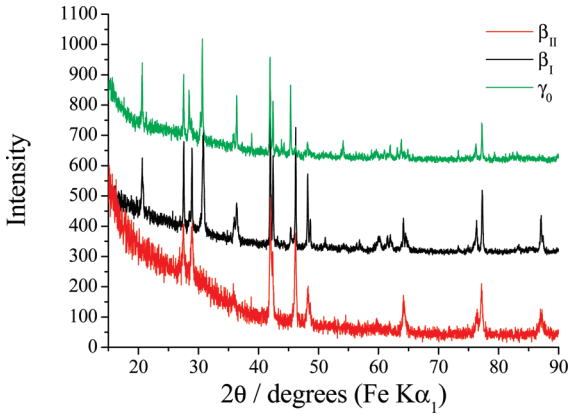

Figure 1. Powder X-ray diffraction patterns for 3 polymorphs of Li_2CoSiO_4.

Time-of-flight powder neutron diffraction data were obtained on the Polaris high-intensity, medium resolution instrument at ISIS at the Rutherford Appleton Laboratory. Since both lithium and, to a lesser extent, cobalt are neutron absorbers, the data were corrected for absorption. The structures were refined by the Rietveld method using the program TOPAS Academic.[13]

The three polymorphs were characterized by ^{7}Li MAS NMR at ICMCB, using a Bruker Avance 300 MHz spectrometer with 2.5 mm rotors spinning at 30 kHz. A combination of single pulse and Hahn echo experiments was used with a 90° pulse duration of 1.2 μs. The recycle time was varied to allow full relaxation.

Results

Powder X-ray diffraction patterns of the three Li_2CoSiO_4, polymorphs β_{II}, β_I and γ_0, prepared as described in the Experimental Section are presented in Figure 1.

Neutron Diffraction. Powder diffraction data for the as-prepared product of hydrothermal synthesis could be indexed on the basis of a primitive orthorhombic unit cell, space group $Pmn2_1$. According to the notation of West and Glasser this represents the β_{II} polymorph.[8a] Rietveld refinement of the powder neutron diffraction data using this space group gave an excellent fit with R_{wp} of 1.63%. However, instead of the ideal β_{II} cation arrangement with all the Co in the 2a tetrahedral sites and Li in 4b sites, pronounced disorder was observed. The transition metal 2a site is effectively exclusively occupied by lithium, while the 4b site is approximately equally occupied by lithium and cobalt. This gives a site in which the average neutron scattering length is close to zero, giving poor definition of the cation position. Accordingly, a combined X-ray and neutron refinement was carried out to give better characterization of this 4b site. Final refined parameters are shown in Table 1, and the fit to the neutron data is shown in Figure 2a. The final refined composition corresponds to $Li_{1.96}Co_{1.04}SiO_4$, within 2 e.s.d.s of the ideal stoichiometry. As indicated above the β polymorphs all exhibit corner shared tetrahedra, aligned such that the vertices point along the c direction. In β_{II} Li_2CoSiO_4 chains of the Li/Co tetrahedra run along the a direction parallel to chains of alternating

(10) West, A. R. *Z. Kristallogr.* **1975**, *111*, 422.
(11) (a) Yamaguchi, H.; Akatsuka, K.; Setoguchi, M.; Takaki, Y. *Acta Crystallogr., Sect. B: Struct. Crystallogr. Cryst. Chem.* **1979**, *35*, 2680. (b) Politaev, V. V.; Petrenko, A. A.; Nalbandyan, V. B.; Medvedev, B. S.; Shvetsova, E. S. *J. Solid State Chem.* **2007**, *180*, 1045. (c) Jousseaume, C.; Kahn-Harari, A.; Vivien, D.; Derouet, J.; Ribot, F.; Villain, F. *J. Mater. Chem.* **2002**, *12*, 1525. (d) Riekel, C. *Acta Crystallogr., Sect. B: Struct. Crystallogr. Cryst. Chem.* **1977**, *33*, 2656.
(12) Arroyo-de Dompablo, M. E.; Dominko, R.; Gallardo-Amores, J. M.; Dupont, L.; Mali, G.; Ehrenberg, H.; Jamnik, J.; Moran, E. *Chem. Mater.* **2008**, *20*, 5574.
(13) Coelho, A. A. *J. Appl. Crystallogr.* **2000**, *33*, 899.

Table 1. Refined Crystallographic Parameters for β_{II} Li_2CoSiO_4, Space Group $Pmn2_1$[a]

atom	Wyckoff symbol	*x*/*a*	*y*/*b*	*z*/*c*	B_{iso}	occupancy
Li1	2a	0	0.1515(18)	−0.0121(19)	0.94(19)	1
Si1	2a	0.5	0.1743(7)	0	0.50(3)	1
Li2/Co1	4b	0.264(4)	0.293(4)	0.442(6)	0.3(-)	0.48/0.52(1)
O1	4b	0.2839(3)	0.3180(4)	0.9070(8)	0.60(2)	1
O2	2a	0	0.1164(4)	0.4004(11)	0.47(3)	1
O3	2a	0.5	0.1789(6)	0.3362(8)	0.74(3)	1

[a] R_e = 1.46%, R_{wp} = 1.63%, R_p = 2.70%, a = 6.2558(2) Å, b = 5.3584(2) Å, c = 4.9357(2) Å.

LiO_4 and SiO_4 tetrahedra. Bond lengths and angles are shown in Table 4.

By heating the as-prepared material to 700 °C for 2 h a polymorph with double the lattice parameter along the *b* direction is obtained. Powder diffraction data for this phase could be indexed in space group $Pbn2_1$. A Li_2CoSiO_4 phase adopting this space group was previously reported by Yamaguchi et al., who described it as the β_{II} polymorph.[11a] However, using the notation of West and Glasser, this should more properly be designated β_I. Rietveld refinement of the powder neutron diffraction data, using starting coordinates from Yamaguchi et al., gave an excellent fit with R_{wp} of 1.77%. A small degree of site disorder was observed with 2.4(16) % Li on the Co site and 8.6(14) % Co on one of the two Li sites. Final refined parameters are shown in Table 2, and the fit to the data is shown in Figure 2b. Again the final refined composition corresponds to $Li_{1.94}Co_{1.06}SiO_4$, within 2 e.s.d.s of the ideal stoichiometry. While the tetrahedra are again all aligned along the *c* direction, they are ordered in a different manner. There are chains of alternating LiO_4 and CoO_4 tetrahedra along *a*, parallel to chains of alternating LiO_4 and SiO_4 tetrahedra. Bond lengths and angles are given in Table 5.

The product of heating the β_{II} polymorph to 1100 °C with quenching from 850 °C generated a third polymorph (γ_0). This is also characterized by a lattice doubling along the *b* direction and can be indexed in the monoclinic space group $P2_1/n$. Once more Rietveld refinement of the powder neutron diffraction data gave an excellent fit with R_{wp} of 1.62%. No site disorder was observed for this polymorph. Final refined parameters are shown in Table 3, and the fit to the data is shown in Figure 2c. In the γ polymorphs the tetrahedra are arranged in groups of 3 with the central tetrahedron pointing in the opposite direction to the outer 2, with which it shares edges. In γ_o Li_2CoSiO_4 this group of 3 edge-sharing tetrahedra consists of Li−Li−Co. Bond lengths and angles are given in Table 6.

Figure 3 shows schematic representations of the structures of the 3 polymorphs revealing the different connectivity.

NMR. The full ^{7}Li MAS NMR spectra for the three polymorphs are shown in Figure 4. Integration of the whole signal (including the spinning sidebands) leads to very similar amounts of Li per mass of sample for the three polymorphs. Although one cannot exclude the possibility that the T2 relaxation time could be different for the three polymorphs, this suggests that all the Li are observed in the three cases. Most isotropic signals are strongly negatively shifted due to Fermi contact interaction from the paramagnetic Co^{2+} ions present in the structure.

NMR Shifts − Background. ^{7}Li NMR Fermi contact shifts are due to the transfer of some density of electron spins to the site of the Li nucleus from the orbitals of a neighboring ion carrying unpaired electrons. Based on earlier Li NMR characterization of Li-transition metal oxides and DFT modeling of the electron spin distribution, the transfer mechanisms elucidated so far can be described as follows.[14]

If a d orbital carries an unpaired electron spin, it aligns with the applied field. If this orbital can overlap with the 2s orbital of Li, either directly 2s-nd (like a spin in a t_{2g} orbital of an octahedral transition metal ion with a Li in an edge-sharing octahedron) or via p orbitals of O 2s-O2p-nd (like a spin in an e_g orbital of an octahedral transition metal ion with a Li in a corner-sharing octahedron), a delocalization mechanism operates, and Li receives a density of unpaired spin with the same polarization. This leads to a positive Fermi contact shift.

A fully occupied d orbital (therefore carrying no unpaired spin) can be polarized by unpaired spins in another (higher energy) d orbital of the same transition metal ion that carries unpaired spins (parallel to the applied field). This polarization consists in a separation (in space and in energy) of the two otherwise paired spins. The spin (from the pair) with the same orientation as that of the unpaired spin in the other orbital is attracted by this unpaired spin. Therefore, the spin (from the pair) with the opposite orientation is more spread out in the orbital. If this polarized orbital overlaps with the 2s of Li, again either directly or via oxygen, Li receives a density of spin with opposite orientation to the applied field. This leads to a negative Fermi contact shift. One such case is e_g spins for an octahedral transition metal ion that polarize full t_{2g} orbitals; the latter can overlap with an edge sharing octahedral Li. Another case is electron spins in a (nonbonding) t_{2g} orbital that polarize the bonding counterpart of an empty antibonding e_g (that should actually be called e_g*). This polarized bonding e_g orbital can overlap via O with a Li in a corner-sharing octahedron.

This is relatively straightforward in octahedral coordination where the e_g orbitals point to the oxygens and the t_{2g} orbitals point to the edges, and the Li in edge or corner sharing octahedra are ideally placed to interact with these

(14) (a) Carlier, D.; Ménétrier, M.; Grey, C. P.; Delmas, C.; Ceder, G. *Phys. Rev. B* **2003**, *67*, 174103. (b) Chazel, C.; Ménétrier, M.; Carlier, D.; Croguennec, L.; Delmas, C. *Chem. Mater.* **2007**, *19*, 4166.

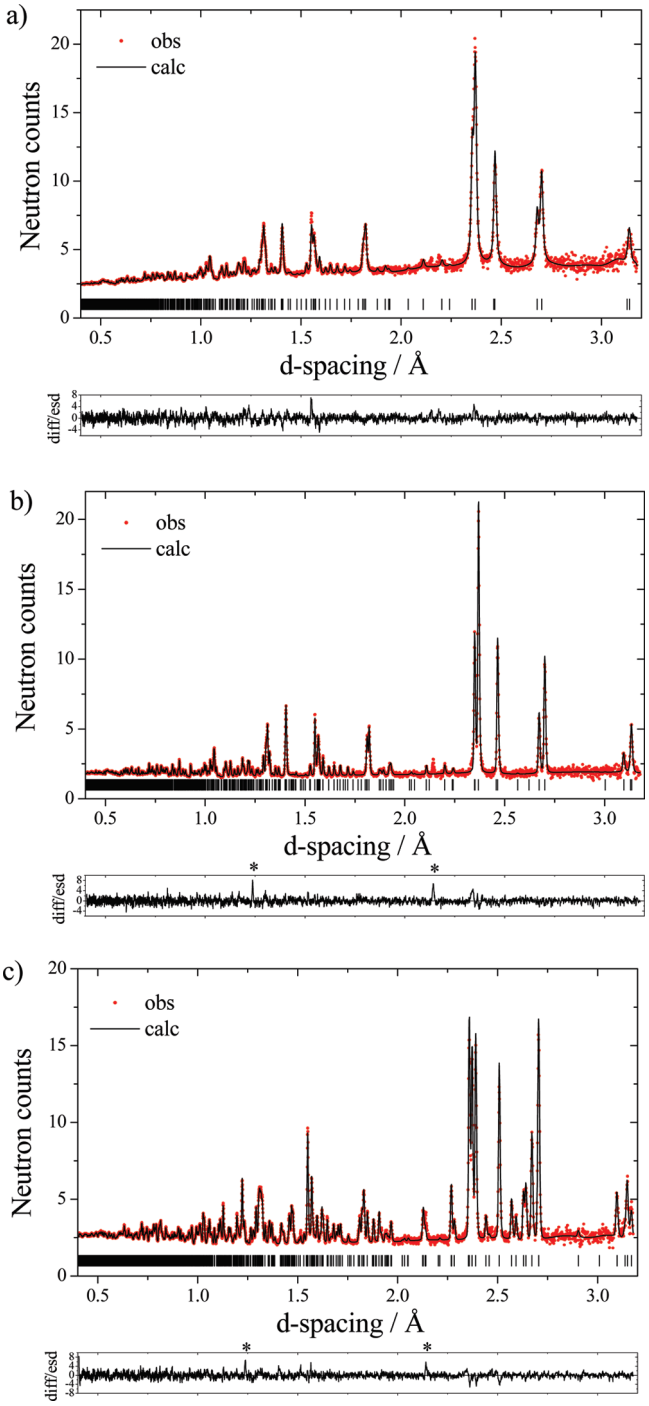

Figure 2. a) Refined powder neutron diffraction pattern for as-synthesized β_{II} Li_2CoSiO_4, space group $Pmn2_1$. b) Refined powder neutron diffraction pattern for as-synthesized β_I Li_2CoSiO_4, space group $Pbn2_1$. c) Refined powder neutron diffraction pattern for as-synthesized γ_0 Li_2CoSiO_4, space group $P2_1/n$. Dots represent observed data and solid line the calculated pattern. The lower line is the difference/esd. The misfit in a) arises from stacking faults, while asterisks in b) and c) denote reflections from the vanadium sample holder.

orbitals. However, in tetrahedral coordination for the transition metal ion and for Li, the e and t_2 orbitals point, respectively, toward the edges (perpendicularly) and to the faces (not perpendicular to a face but parallel to two of the opposite edges) of the tetrahedron, and the Li in adjacent tetrahedra are not in obvious positions to overlap with these orbitals.

Following these rules of thumb, the shifts expected for the Li_2CoSiO_4 polymorphs can nevertheless be tentatively discussed as follows.

Cobalt has an oxidation state +2 in these compounds, and its electronic configuration in a tetrahedron is therefore $e^4\ t_2^3$ (the e orbitals are fully occupied, while each t_2 orbital contains one unpaired spin).

In the β polymorphs, the nature of the connection of any tetrahedral Li site with the surrounding ones containing Co is represented in Figure 5. The Co tetrahedra present either face-to-face, face-to-edge, or edge-to-face connection relative to the Li tetrahedron. Following the rules just expressed, a Co^{2+} ion with a face-to-face connection would have t_2 orbital lobes pointing toward this Li through the facing faces of the tetrahedra (face-to-face geometry); and one would expect the transfer of an electron spin density aligned with the applied field, leading to a positive Fermi contact shift. A similar situation arises for the face-to-edge connection (the orbital exiting from the face now points to Li through the edge of its tetrahedron). Finally, for the edge-to-face connection the fully occupied but polarized e orbital points from the edge but perpendicularly, in such a way that it is not directed toward the Li tetrahedron, and the latter should not receive significant electron spin density with polarization opposite to the applied field.

The experimental shifts in these polymorphs are however clearly negative (Figure 4). There is therefore a polarization mechanism not taken into account in our discussion. This most probably operates via the oxygens, through bonding counterparts of the e and t_2 orbitals discussed so far. If these bonding (mostly of O character) orbitals are polarized by the spin-carrying t_2 orbital, they must transfer an electron spin density leading to a negative Fermi contact shift via the O, superseding the direct overlap of the t_2 orbital through the faces. The precise interplay and respective geometries of the t_2 orbital and of the bonding ones remains to be studied in detail in a tetrahedral coordination.

As concerns the γ_0 polymorph, the same type of connection between the tetrahedra occurs (although with considerable distortion in the alignment of the tetrahedral) (Figure 6), but edge-sharing also occurs in addition, as discussed in the Introduction and shown in Figure 6. In this configuration, a polarized e orbital from Co should point directly to Li through the common edge, contributing a negative Fermi contact shift that could explain the negative shift for one of the Li sites.

Despite this lack of global understanding of the spin transfer mechanism, we can still analyze the NMR signals in terms of number of signals with respect to the possible local environments due to the actual Li/Co site distribution deduced from the Rietveld analyses.

β_{II} Polymorph. The Li (2a) site (Figure 6) is surrounded by 4 (0.52Co/0.48Li) tetrahedra with a face-to-face geometry; this should lead to a distribution of 5 resonances, out of which 3 have significant magnitudes ((1:2:3 Co) with probabilities (0.23:0.37:0.27)). The remaining two have probabilities much lower than 0.10. In addition, the

Table 2. Refined Crystallographic Parameters for β_I Li_2CoSiO_4, Space Group $Pbn2_1$[a]

atom	Wyckoff symbol	*x*/*a*	*y*/*b*	*z*/*c*	B_{iso}	occupancy
Co1	4a	0.5005(17)	0.1652(9)	0.253(3)	0.61(11)	Co/Li 0.976/0.024(16)
Si1	4a	0.2494(13)	0.4130(3)	0.25(-)	0.33(3)	1
Li1	4a	−0.019(3)	0.1638(13)	0.251(4)	0.4(2)	Li/Co 0.914/0.086(14)
Li2	4a	0.741(3)	0.4217(7)	0.2402(13)	0.77(9)	1
O1	4a	0.0337(6)	0.3425(4)	0.1478(9)	0.33(6)	1
O2	4a	0.2542(10)	0.55780(14)	0.1459(6)	0.39(2)	1
O3	4a	0.2451(10)	0.4106(2)	0.5811(5)	0.30(2)	1
O4	4a	0.4660(6)	0.3417(5)	0.1396(7)	0.39(5)	1

[a] R_e = 1.61%, R_{wp} = 1.77%, R_p = 3.00%, *a* = 6.25990(10) Å, *b* = 10.6892(2) Å, *c* = 4.92866(8) Å.

Table 3. Refined Crystallographic Parameters for γ_0 Li_2CoSiO_4, Space Group $P2_1/n$[a]

atom	Wyckoff symbol	*x*/*a*	*y*/*b*	*z*/*c*	B_{iso}	occupancy
Co1	4e	0.4968(8)	0.1656(4)	0.3074(7)	0.37(4)	1
Si1	4e	0.2480(4)	0.41233(14)	0.3135(4)	0.13(2)	1
Li1	4e	−0.0047(10)	0.1631(6)	0.3072(10)	0.51(6)	1
Li2	4e	0.2385(11)	0.0760(4)	0.7145(10)	0.86(6)	1
O1	4a	0.2475(3)	0.40939(14)	0.6381(3)	0.350(14)	1
O2	4a	0.2539(3)	0.55630(12)	0.2071(3)	0.41(2)	1
O3	4a	0.0334(3)	0.3409(2)	0.2081(3)	0.36(2)	1
O4	4a	0.4604(3)	0.3400(2)	0.2079(3)	0.34(2)	1

[a] R_e = 1.33%, R_{wp} = 1.62%, R_p = 2.89%, *a* = 6.27433(10) Å, *b* = 10.6854(2) Å, *c* = 5.01631(9) Å, β = 90.600°(2).

Table 4. Refined Bond Lengths and Angles for β_{II} Li_2CoSiO_4, Space Group $Pmn2_1$

Li1O4	O1	O1	O2	O3
O1	2.028(5)	122.4(5)	103.7(3)	109.2(3)
O1		2.028(5)	103.7(3)	109.2(3)
O2			2.044(11)	107.7(5)
O3				1.922(10)
SiO4	**O1**	**O1**	**O2**	**O3**
O1	1.622(3)	112.9(3)	111.6(2)	106.0(2)
O1		1.622(3)	111.6(2)	106.0(2)
O2			1.633(5)	108.4(3)
O3				1.660(4)
(Li/Co)O4	**O1**	**O1**	**O2**	**O3**
O1	2.113(2)	91.8(9)	111.0(11)	117.2(13)
O1		2.305(3)	100.5(11)	106.3(12)
O2			1.912(2)	123.1(13)
O3				1.682(2)

same Li is also surrounded (Figure 7) by two (0.52Co/0.48Li) tetrahedra with a face-to-edge-geometry and two with an edge-to-face geometry. This should lead to a further splitting of each of the resonance just mentioned into 9 resonances with rather similar magnitudes (probabilities ranging from 0.05 to 0.19).

The Li/Co site (0.48Li/0.52Co) (Figure 8) is surrounded by 4 (0.52Co/0.48Li) tetrahedra (2 face-to-face, 1 face-to-edge, 1 edge-to-face). This should lead to a distribution of 12 resonances with rather similar magnitudes (probabilities from 0.05 to 0.13). Altogether, the distribution of resonances for the two crystallographic types of Li is therefore expected to be very broad.

The experimental pattern (Figure 9) is in good agreement with this. It shows a set of at least two broad resonances, but, not knowing the value of the shift caused by each Co in each possible environment, one cannot infer that these two apparent signals correspond to the two crystallographic sites. It is more likely that for a given crystallographic site the very broad distribution in the possible number of Co leads to a set of signals contributing within the whole ppm range. For both types of Li, among all the possibilities is the one having zero adjacent Co; such a configuration occurs statistically for 5% of the Li in 2a and for 5% of the 0.48 Li in Li/Co site. It is reasonable to assume that these environments lead to the contribution observed around 0 ppm in the spectrum. Besides, it is interesting to note that contributions with positive shifts are also present in the overall spectrum. These may correspond to cases where the delocalization mechanisms mentioned above are not overtaken by a polarization via O. Improvement of the modeling of these interaction mechanisms is clearly needed in this respect.

β_I Polymorph. The Li site (containing 0.91Li) is surrounded as in Figure 4 by four tetrahedra containing 0.98 Co: two with a face-to-face geometry, one with a face-to-edge geometry, and one with an edge-to-face geometry. This should lead to a distribution of 12 signals

Table 5. Refined Bond Lengths and Angles for β_I Li_2CoSiO_4, Space Group $Pbn2_1$

CoO4	O1	O2	O3	O4
O1	1.957(16)	108.5(6)	109.7(6)	109.4(6)
O2		2.036(12)	105.7(6)	112.2(6)
O3			1.928(13)	111.3(6)
O4				1.980(11)
SiO4	O1	O2	O3	O4
O1	1.625(8)	111.0(4)	106.9(4)	111.5(3)
O2		1.631(3)	109.2(2)	108.6(4)
O3			1.632(2)	109.6(4)
O4				1.650(8)
Li1O4	O1	O2	O3	O4
O1	2.004(16)	109.0(8)	114.8(9)	107.0(8)
O2		2.074(16)	106.6(8)	105.9(8)
O3			1.876(18)	113.3(9)
O4				1.916(22)
Li2O4	O1	O2	O3	O4
O1	2.062(17)	104.8(7)	104.6(7)	122.5(4)
O2		2.012(7)	107.3(3)	107.7(7)
O3			1.958(7)	109.2(7)
O4				1.992(17)

Table 6. Refined Bond Lengths and Angles for γ_0 Li_2CoSiO_4, Space Group $P2_1/n$

CoO4	O1	O2	O3	O4
O1	1.965(5)	112.8(2)	109.4(2)	111.9(2)
O2		1.960(5)	95.7(2)	118.0(2)
O3			2.022(4)	107.5(2)
O4				1.942(5)
SiO4	O1	O2	O3	O4
O1	1.629(2)	110.25(12)	107.72(14)	108.98(14)
O2		1.629(2)	110.94(16)	108.61(16)
O3			1.631(3)	110.31(13)
O4				1.633(3)
Li1O4	O1	O2	O3	O4
O1	1.926(6)	113.4(3)	112.0(3)	109.6(3)
O2		1.946(6)	117.0(3)	97.1(3)
O3			1.979(7)	106.3(3)
O4				2.025(6)
Li2O4	O1	O2	O3	O4
O1	1.930(5)	106.8(2)	111.6(3)	117.7(3)
O2		1.946(6)	89.9(2)	93.3(23)
O3			2.053(6)	127.1(2)
O4				1.962(7)

corresponding to Li with different numbers of Co neighbors in different positions, but one signal (the one with 4 Co) should dominate (92% of total magnitude, the others representing less than 4%).

The Li2 site, with a Li occupancy of 1, is similarly surrounded by 0.98 Co sites, leading to a similar distribution of signals. In addition, this Li2 site also is similarly surrounded by 0.09 Co (Li1) sites that further splits each of these 12 resonances into a distribution of 12, of which the major one is 0 Co and corresponds to 69% of the total (the rest less than 14%).

The 0.02 Li present in the 0.98 Co site do not have any connection with a Co-rich site. However, again they have the same type of surrounding as shown in Figure 4 with the 0.09 Co tetrahedra. This again leads to a distribution of 12 resonances for this 0.02 Li, the major one being the one with 0 Co corresponding to 69% of the total (the others are less than 14%). These 0.02×0.69 Li should resonate at 0 ppm since they do not have any connection to a Co tetrahedron.

The NMR spectrum of the β_I polymorph (Figure 10) exhibits three well-defined signals; following the analysis described above, they can tentatively be assigned as shown in the figure. The other resonances would be too distributed to be identified, although they should account for 25% of the total amount of Li. In addition, a very weak narrow signal close to -1.5 ppm most probably corresponds to an unidentified diamagnetic impurity. Integration of the spectra over all the spinning sidebands, compared to the relative magnitudes expected from this

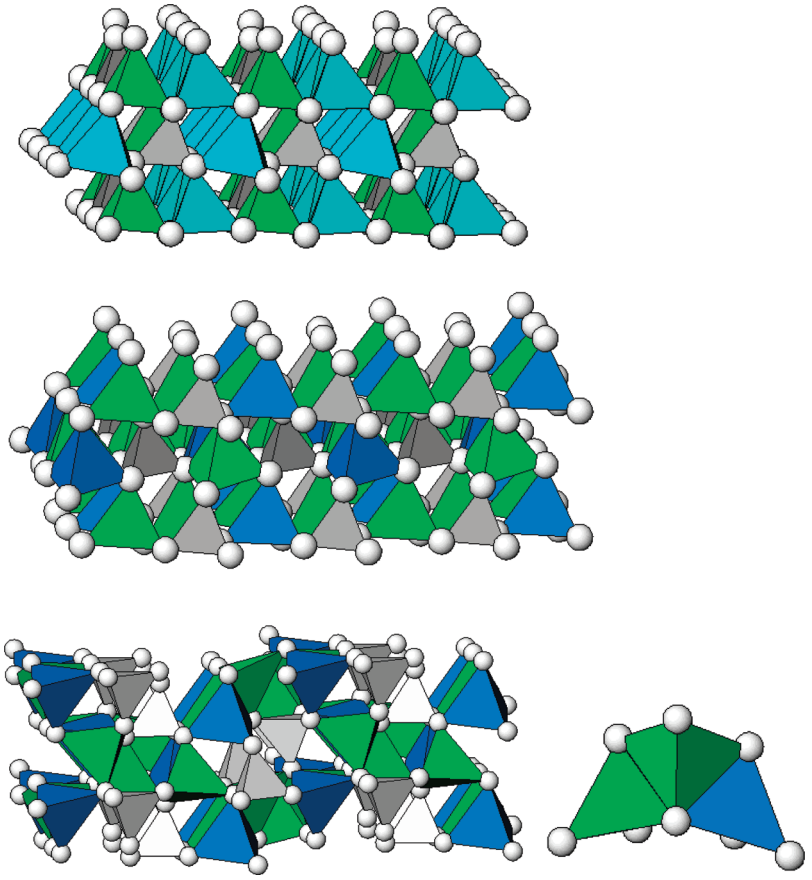

Figure 3. Schematic representations of the three Li_2CoSiO_4 polymorphs. **a**) β_{II}, **b**) β_I, and **c**) γ_0, with the inset showing edge sharing tetrahedra. Gray tetrahedra represent SiO_4, green LiO_4, blue CoO_4, and cyan $(Li,Co)O_4$.

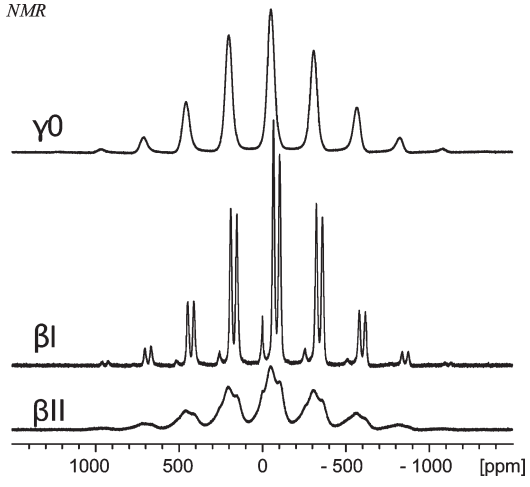

Figure 4. ^{7}Li MAS NMR spectrum of the three polymorphs of Li_2CoSiO_4 (116 MHz, 30 kHz spinning, Hahn echo). The absolute magnitude scale referred to the mass of the samples.

assignment, is shown in Table 7. The 0 ppm signal is clearly too intense for this assignment, which would imply more Li in the Co site (or less Co in the adjacent 0.91Li/0.09Co site). This might however also partly be due to difficulties in subtracting the narrow additional component in the spectral decomposition for integration and to the influence of the additional unresolved distribution of signals representing 25% of the total amount of Li.

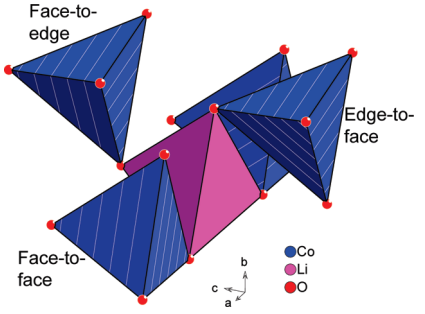

Figure 5. Schematic representation of the surrounding of Li by Co in the beta polymorphs.

γ_0 Polymorph. In the γ_0 polymorph there is no Li/Co mixing according to the Rietveld results reported in this paper, so that only one resonance is expected for each Li site.

The Li in the Li1 site (Figure 6) is connected to four Co tetrahedra with globally the same geometry as in the other two polymorphs (2 face-to-face, 1 face-to-edge, 1 edge-to-face). However, the arrangement of the tetrahedra is so distorted that one can hardly expect the t_2 or the polarized e orbitals of Co to point toward this Li.

The Li in the Li2 site (Figure 6) has a quite different environment, since, in addition to "face-to-face" connection with two Co tetrahedra, it also shares one edge with a Co tetrahedron. Following the mechanisms discussed in this paper, this is an ideal situation

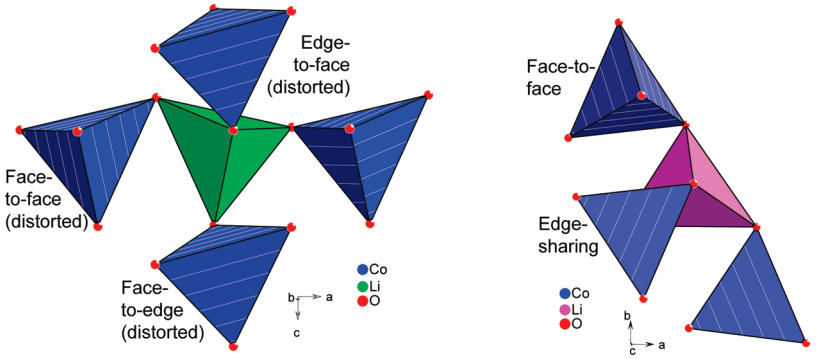

Figure 6. Schematic representation of the surrounding of the two types of Li by Co in the gamma 0 polymorph.

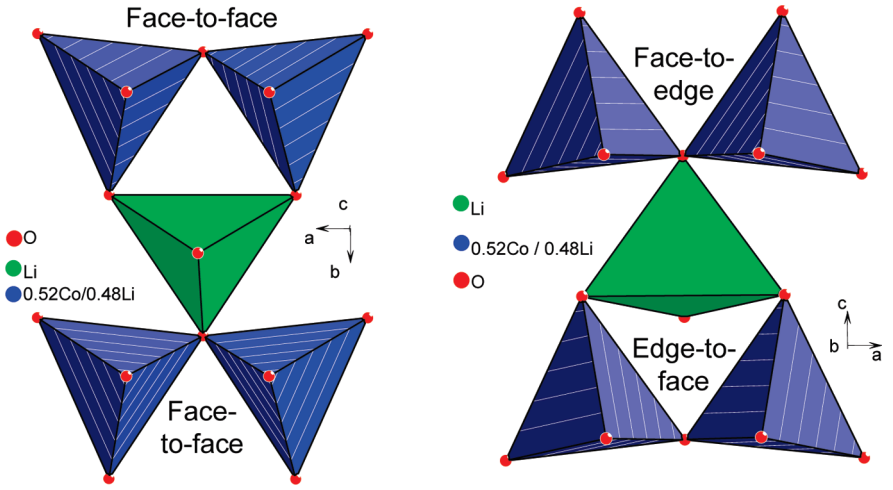

Figure 7. Surrounding of one type of Li (2a site) by Co in the β_{II} polymorph.

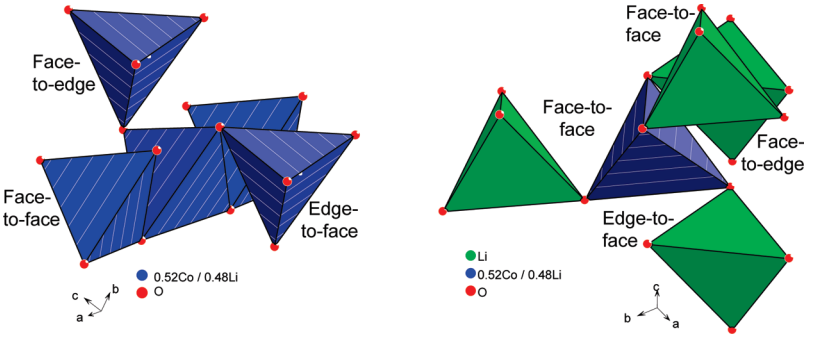

Figure 8. Surrounding of the Li/Co(4b) sites in the β_{II} polymorph.

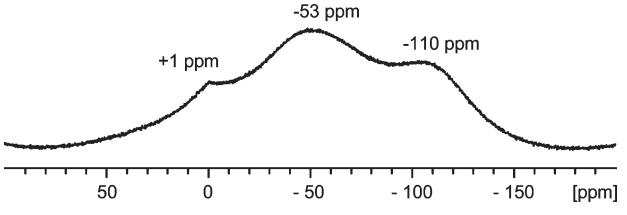

Figure 9. ^{7}Li MAS NMR spectrum (isotropic signals) of the β_{II} polymorph (116 MHz, 30 kHz spinning, Hahn echo).

for a negative shift due to transfer of electron spin density from the polarized e orbital, although Li2 appears quite off-centered in its tetrahedron (Figure 11).

The ^{7}Li NMR spectrum of the γ_0 polymorph (Figure 12) however shows a single resonance with a 58% Gaussian − 42% Lorentzian line shape. Variable temperature (cooling to about 250 K), ^{6}Li resonance at 44.2 MHz, or ^{7}Li resonance at 38.9 MHz with a 30 kHz spinning did not lead to any sign of splitting of this signal. Not knowing the shift mechanisms in this system, we cannot exclude the possibility that the shifts for the two types of Li happen to coincide, although this appears somewhat unlikely for such different environments. Besides, the width of the line (as compared to the other 2 polymorphs) would rather suggest a distribution of signals that should result from some kind of Li/Co exchange.

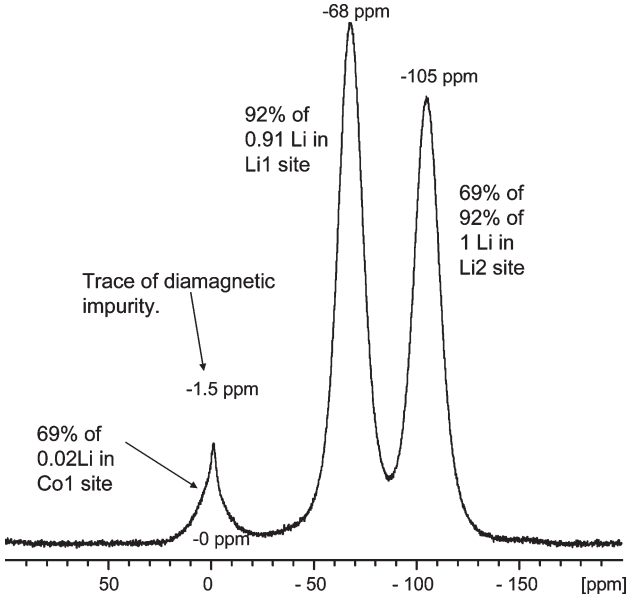

Figure 10. ^{7}Li MAS NMR spectrum (isotropic signals) of the β_I polymorph (116 MHz, 30 kHz spinning, Hahn echo).

Table 7. Relative Magnitude of the ^{7}Li NMR Signals in the β_I Polymorph Compared to the Values Expected Based on the Analysis Described in the Text

signal	0 ppm	−68 ppm	−105 ppm
expected magnitude %	0.9	56.3	42.7
integration %	5.8	48.43	45.53

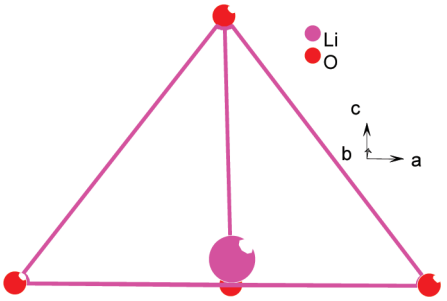

Figure 11. Open view of the Li(2)O_4 tetrahedron.

Conclusion

Li_2CoSiO_4 was prepared in three pure polymorphic forms (β_{II}, β_I, and γ_0) as described previously.[7g] Rietveld refinement of X-ray and neutron powder diffraction patterns demonstrated a considerable Li/Co mixing for β_{II} with close to 50/50 occupation in the 4b site. Very moderate mixing in the Co site (2.4% Li) and one of the Li sites (8.6% Co) was observed for the β_I polymorph, and no mixing was found for γ_0. ^{7}Li MAS NMR spectra were recorded for all 3 polymorphs. The mechanism of the Fermi contact interaction that leads to the observed negatively shifted signals cannot be explained based on our present understanding. A polarization-type mechanism involving bonding orbitals with O character seems to overwhelm the expected delocalization mechanism from the t_2 orbitals of tetrahedral Co^{2+} ions that carry the unpaired spins. However, the nature and the number of signals were analyzed in relation with the site occupancies for each compound. Very poorly defined signals are obtained for β_{II}, in good agreement with the considerable extent of disorder expected from the diffraction results. For β_I, well-defined NMR signals can be assigned to definite environments, in reasonable (although not fully quantitative) agreement with the expected structure and site occupancies. Finally, the γ_0 sample surprisingly leads to a single rather broad NMR signal, whereas two well-defined and rather different environments are present in the structure deduced from diffraction.

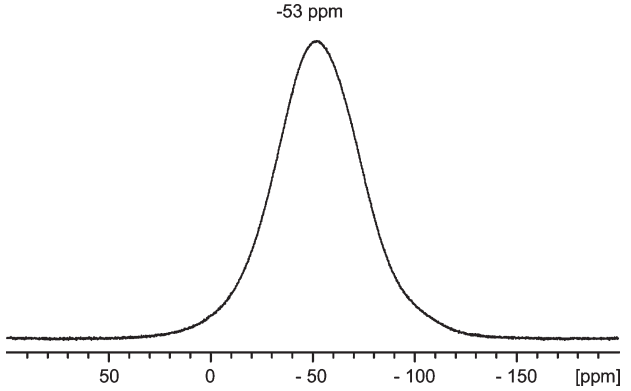

Figure 12. ^{7}Li MAS NMR spectrum (isotropic signal) of the γ_0 polymorph (116 MHz, 30 kHz spinning, Hahn echo).

Acknowledgment. We thank Dany Carlier for fruitful discussions. Peter G. Bruce is indebted to EPSRC for financial support.